Green Chemistry

Accepted Manuscript

ROYAL SOCIETY OF CHEMISTRY

www.rsc.org/greenchem

Journal Name

ARTICLE

Synergism in semiconducting nanocomposite: Visible light photocatalysis towards formation of C-S and C-N bonds

Received 00th January 20xx,
Accepted 00th January 20xx

DOI: 10.1039/x0xx00000x

www.rsc.org/

Anil R. Wade, Hari R. Pawar, Megha V. Biware and Rajeev C. Chikate*

A simple, facile and visible light driven photochemical synthesis of 2-substituted benzothiazoles and 2-substituted benzimidazoles is achieved with CdSe nanocomposites as a photocatalyst. These nanocomposites are prepared by molecular self assembly of 2 – 3 nm sized Zinc blend CdSe phase within the layers of montmorillonite (MMT) through intercalation forming lamellar structure. CdSe/MMT exhibit excellent photocatalytic activity towards synthesis of benzazoles with aliphatic, aromatic and heterocyclic aldehydes with better yields and the efficiency is retained up to five cycles. XRD, XPS and Raman analyses of fresh and used CdSe/MMT reveal the passivation of structural defects due to formation of thin layer of CdO on the photocatalyst surface. Mixed phase of CdSe-CdO facilitates the generation of hetero-junction on CdSe/MMT surface which is beneficial for photostability and sustainability. This process is also highly efficient under solar light and provides easy product isolation on gram scale and therefore, may be regarded as greener methodology for the synthesis of bioactive scaffolds with excellent yields and high chemoselectivity using tailored-made photocatalyst.

Introduction

In recent past, efficient harvesting and effective utilization of solar energy through photocatalytic process has become a prime aspect of various scientific developments.[1] It has encouraged several researchers to investigate visible light driven organic transformations using a heterogeneous catalyst that afford high yield of desired product with minimum leaching of catalyst.[2] Such a pragmatic shift has arisen due to ever increasing environmental concerns as conventional chemical processes utilize hazardous reagents that ultimately generate secondary toxic wastes. Photocatalysis is a process that explores the potentiality of a photocatalyst, besides absorbing light, it can efficiently bring about the organic transformation with high selectivity.[3] It spans the large spectrum of applications that include environmental remediation of aquatic pollutants,[4] splitting of H_2O for generation of H_2,[5] photochemical reduction of CO_2,[6] solar cells[7] that are considered as clean, green and eco-friendly as well as sustainable alternative processes. One such area that has been explored extensively centers around visible light induced activation of C-H[8] bond as well as C-C,[9] C-N[10] or C-S[11] bond formation through photogenerated radicals in presence of a photocatalyst. Designing of tailor-made photocatalyst is a key towards improved quantum efficiency and its subsequent utilization in these processes. This strategy may be achieved via tuning the band gap of semiconducting nanoparticles and dispersing them in a media thereby forming a heterogenized nanocomposite.

There are several advantages of nanocomposites: (i) increased surface area, (ii) generation of distinct reactive sites that are beneficial for efficient absorption of visible light, (iii) uniform dispersion of nanoparticles within solid support hinders their agglomeration, (iv) electron-hole recombination may be suppressed, (v) strong adsorption capacity of support improves the substrate-photocatalyst interaction via adsorption thereby enhancing the rate of photochemical reaction, (vi) photo-corrosion of photocatalyst surface may be inhibited and therefore, these catalysts can be used successfully for subsequent reactions without compromising with their photocatalytic efficiency.[12] These facets result in the development of synergism in nanoparticle-support interactions through formation of a bi-functional photocatalyst that possess desired photocatalytic activity for beneficial applications.

To investigate this hypothesis, we have designed a photocatalyst that comprises of CdSe nanoparticles (NP's) dispersed in montmorillonite (MMT) clay matrix and evaluated its activity towards visible light assisted organic transformations. Three aspects are envisaged: (i) CdSe being an n-type semiconductor with a band gap (1.65 – 1.8 eV)[13] in the visible region can efficiently function as light harvesting site (ii) formation of lamellar structure with MMT[14] and (iii) beneficial adsorption capacity and presence of acidic sites on MMT may enhance the rate of photochemical reaction.

Nanoscience Group, Department of Chemistry, Post-graduate & Research Center, MES Abasaheb Garware College, Pune-411004, India
Email: rajuchikate29@gmail.com, Fax: +91-20-25438165; Tel: +91-20-41038263.
[a]† Footnotes relating to the title and/or authors should appear here.
Electronic Supplementary Information (ESI) available: Scheme of synthesis, PL spectra, Compositional analysis of catalyst, NMR spectra and spectral data
DOI: 10.1039/x0xx00000x

Although toxic effects of CdSe NP's are of major concern to environment and human beings, their cytotoxicity can be controlled through their surface modification and formation of core-shell structure. Due to formation of such a tailored-made nanocomposite, it is expected that the association of CdSe NP's and MMT would generate synergism in their bonding and result in better photocatalytic activity towards organic transformation. Moreover, MMT is inexpensive, thermally and chemically stable and the photochemically inert material. This proposition is evaluated for visible light induced photochemical synthesis of two model compounds *viz*. benzimidazole and benzothiazole.

Benzimidazoles and benzothiazoles; N-containing heterocylic derivatives, exhibit broad range of biological activities that include antitumor,[15] antiulcer,[16] anti-HIV[17] and antihypertensive.[18] These compounds are commonly synthesized by condensation of aryl 1,2-diamines/thioamine with either carboxylic acids in presence of an acid or aldehydes with an oxidant. These conversions can be achieved via catalytic route involving various catalysts like PTSA[19], H_2O_2/CAN[20], $FeCl_3$/MMT K-10[21], $ZrOCl_2{\cdot}8H_2O$[22], $Co(OH)_2$/CoO[23], 1,4-benzoquinone[24], Au/CeO_2[25], and nano α-MoO_3/TBHP.[26] Although these methods are efficient, use of stoichiometric excess of reagent, high cost of the catalyst, prolonged reaction time, occurrence of side reactions, severe reaction conditions, strong oxidizing nature of the reagents and selectivity for 2-substituted derivatives are some of the environmental concerns of these protocols. Therefore, it is imperative to design a synthetic strategy that involves eco-friendly approach where the effective utilization of visible light in presence of a catalyst can be conveniently employed for synthesis of 2-substituted benzothiazoles and benzimidazoles. For example, green synthesis of these derivatives is achieved in presence of a dye with visible light.[27] Moreover, visible light induced photocatalytic radical cyclization in presence of $[Ru(bipy)_3]^{2+}$ and O_2 is carried with thioanilides.[28a] These reactions are also reported with heterogeneous photocatalysts such as mesoporous graphite carbon nitride,[29] CdS nanosphere,[30] nano-TiO_2,[31] and Pt@TiO_2.[32]

In the present investigation, we report one-pot methodology that comprises of both condensation and photocyclisation with homogeneously dispersed CdSe NP's in MMT matrix. It is also observed that there exists synergism within photo-nanocomposite framework that enhances the rate of photochemical reaction with quantitative conversion towards 2-substituted benzothiazoles and benzimidazoles.

Experimental

Chemicals

All chemicals were of analytical grade and used as received: Cadmium acetate ($Cd(OAc)_2{\cdot}2H_2O$ (Loba Chemie, UK), Selenium powder (Loba Chemie, UK), Cetyl trimethyl ammonium bromide (CTAB, Sigma Aldrich), Montmorillonite K-10 (Fluka), Sodium borohydride ($NaBH_4$, Loba Chemie, UK), aldehydes, 2-aminothiophenol and o-phenylenediamine (Sigma Aldrich). Pre-coated TLC plates (silica gel 60 F_{254}) and column grade silica gel (mesh 100-200) were purchased from Merck, India.

Pretreatment of MMT

MMT clay was digested with excess 1M NaCl solution for 24 h at 60°C and the solid was filtered, washed with acetone and dried at 50°C. The powder was dispersed in distilled water to prepare the colloidal suspension of clay particles and kept overnight. It was filtered, washed with distilled water and acetone and finally dried under vacuum.

Synthesis of CdSe NP's

0.3 g of $NaBH_4$ in 5 mL water was added to 0.78 g Se in 5 mL water to obtain wine red coloured solution of sodium hydrogen selenide (NaHSe). In other flask, aqueous solution of cadmium acetate (1.3 g in 10 mL water) was mixed with 10 mL CTAB (0.02 M) solution. To this mixture, NaHSe solution was added drop wise with constant stirring at 40 °C and the resulting mixture was kept under stirring for 1 h. Wine red coloured product was centrifuged at 3000 rpm, successively washed with methanol and then dried under vacuum.

Preparation of CdSe/MMT nanocomposite

0.2 g of CdSe NP's was dispersed in 15 mL distilled water and the whole mixture was sonicated for 4 h. This solution was added to an aqueous suspension of 1.8 g Na–MMT in 10 mL of water and the whole mixture was stirred at 40 °C for 2 h. The wine red mixture was filtered, washed successively with distilled water and finally with acetone and the product was dried under vacuum. This resulted in 10% CdSe/MMT nanocomposite and similar procedure was adopted for the preparation of 5% and 15% compositions with appropriate amounts of CdSe NP's and MMT (Supporting information Figure S1).

Characterization

Powder X-ray diffraction (XRD) spectra were recorded on Phillips X'pert MPD X-ray diffractometer using Cu Kα radiation. Transmission electron microscope (TEM) images were obtained on JEOL electron microscope (model 1200X). X-ray photoelectron spectroscopy (XPS) analysis was carried out on a VG Micro Tech ESCA3000 instrument using Mg Kα radiation (photo energy 1253.6 eV). Brunauer–Emmett–Teller (BET) surface area analysis was performed using nitrogen adsorption method with surface analyzer system CHEMBET3000, Quantichrome Instruments, U.S. Raman spectra were recorded on Horiba JY LabRAM HR 800 micro-Raman spectrometer operating at 17 mW and 632.8 nm excitation. Photoluminescence (PL) spectra were recorded on a Hitachi F-4500 fluorescence spectrophotometer with the excitation wavelength of 450 nm. ICP-OES measurements were carried out on Optima 7000 DV ICP-OES Spectrometer (Perkin-Elmer). Tungsten lamp with a power of (35 W) equipped with a cutoff filter (λ > 420 nm) was used as a visible light source. Quantum yields of photochemical reactions were measured using ferrioxalate actinometry (Supporting information). ^{1}H NMR (400 MHz and 500 MHz) and ^{13}C NMR (100 MHz and 125 MHz) spectra of synthesized derivatives were recorded on Bruker AV 400 and AV 500 spectrometers either in $CDCl_3$ or DMSO-d_6.

Chemical shifts are reported in ppm from tetramethylsilane and instrument internally referenced to tetramethylsilane (TMS), chloroform or dimethylsulfoxide signals. Reported data is as follows: chemical shift, multiplicity (s; singlet, d; doublet, t; triplet, q; quartet, m; multiplet, dd; doublet of doublet, br. s.; broad singlet), coupling constants in Hertz (Hz). Melting points were recorded on a melting point apparatus (Mettler Toledo) and were uncorrected.

General procedure for photochemical synthesis of 2-substituted benzothiazole

A mixture of aldehyde (10 mmol), 2-aminothiophenol (10 mmol) and catalyst (5 mg) in ethanol (30 mL) was taken in a 100 mL double-walled quartz photoreactor equipped with water chiller (Supporting information Fig S2) to maintain the temperature of the reaction vessel. The reaction medium was exposed to visible light (35 W Tungsten lamp) for appropriate time under constant stirring at room temperature. After the completion of reaction, the catalyst was separated by centrifugation and the filtrate was concentrated under vacuum. The crude product was purified by column chromatography on silica gel (hexane/ethyl acetate) to yield 2-substituted benzothiazoles.

General procedure for photochemical synthesis of 2-substituted benzimidazole

Similar procedure was adopted for the synthesis of 2-substituted benimidazole with aldehyde (10 mmol), o-phenelynediamine (10 mmol) and catalyst (5 mg) in ethanol (30 mL).

Reusability studies

The recycling experiments were carried out with recovered nanocomposite. After each photochemical reaction, the catalyst was separated by simple centrifugation and then it was successively washed with ethanol and acetone to remove the adsorbed organic compounds. This recovered catalyst was used for subsequent cycles under identical experimental conditions and the products were isolated using column chromatography.

Results and discussion

The synthetic strategy adopted in the present investigation is based on the concept of modification of clay with a surfactant that result in the formation of expanded lamellar structure of clay. Logically, CTAB capped CdSe NP's may be intercalated within layers of MMT structure so as to fabricate an inorganic-organic hybrid material with increased layer spacing of MMT (Supporting information Fig. S1). Such an approach would result in generating distinct reactive sites (CdSe) not only on the MMT surface but also within its layers and it may enhance the photocatalytic efficiency of nanocomposite.

Characterization of nanocomposites

The interaction of MMT with CdSe NP's is characterized using X-ray diffraction studies to ascertain the homogeneous dispersion of nanoparticles within MMT matrix (Fig. 1). It is observed that peak corresponding to layered clay structure of

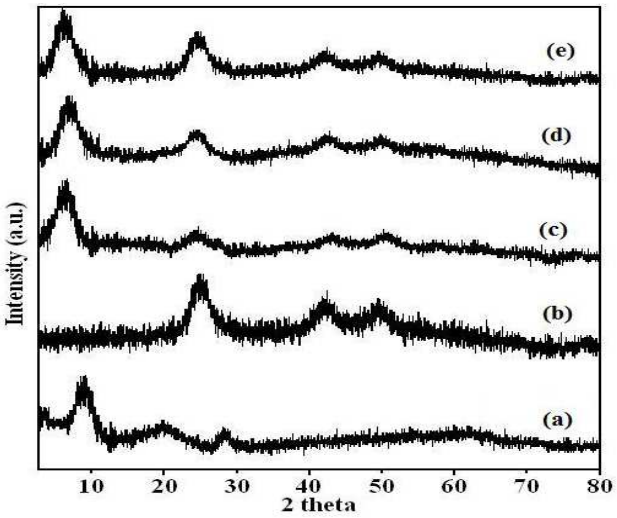

Fig. 1: XRD pattern of CdSe/MMT nanocomposite. (a) MMT, (b) CdSe, (c) 5% CdSe/MMT (d) 10% CdSe/MMT and (e) 15% CdSe/MMT

MMT occurring at 7.8° due to (001) plane is significantly broadened and shifted to lower angle (4.6°) for CdSe/MMT nanocomposite. Such shift attributes to enlargement in the lamellar structure due to insertion of CdSe NP's within MMT layers through intercalation and their uniform distribution in the clay matrix. On the other hand, CdSe region exhibited three characteristics peaks at 25.3°, 42.7° and 50.6° corresponding to (111), (220) and (311) reflections of Zinc blend structure of CdSe NP's (JCPDS file no. 19-0191) which remained unchanged after composite formation with MMT. The spherical shaped CdSe NP's of 2-3 nm size are found to be homogeneously dispersed within layered clay support (Fig. 2).

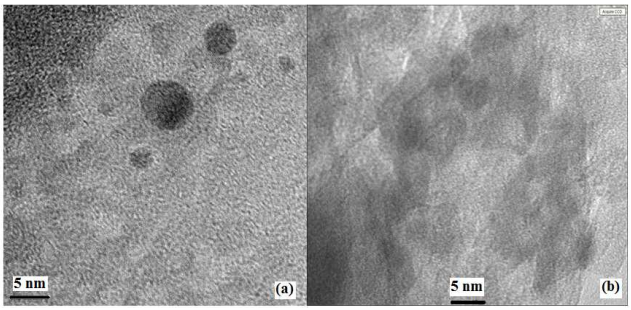

Fig. 2: TEM images of (a) CdSe and (b) 10% CdSe/MMT

The specific surface area of Na–MMT, CdSe NP's, 5% and 10% CdSe/MMT is found to be 34, 24.4, 68.9 and 177.0 m^2g^{-1} respectively. Higher value 10% CdSe doped MMT implies that the nanocomposite formation leads to generation mesoporous structure. CdSe NP's exhibits an emission band at 572 nm while 10% CdSe/MMT composite displays a band at 528 nm (Supporting information Figure S3). The blue shift for composites is probably due to intercalated MMT sheets as well as surface defects inducing dissipation of absorbed energy.

Table 1: Optimized reaction conditions for the synthesis of 2-phenylbenzo[d]thiazole[a]

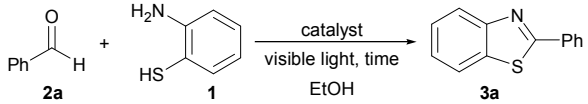

Entry	Catalyst	Amount (mg)	Time (h)	% Yield[b]
1	CdSe NP's	5	0.5	48
2	5% CdSe/MMT	5	0.5	81
3	10% CdSe-MMT	5	0.5	93
4	15% CdSe/MMT	5	0.5	94
5	10% CdSe/MMT	2	0.5	83
6	10% CdSe-MMT	5	0.5	93
7	10% CdSe/MMT	10	0.5	94
8[c]	MMT	5	24	--
9[c,d]	10% CdSe/MMT	5	24	--

[a]Reaction conditions: 10 mmol of 2-aminothiophenol, 10 mmol of benzaldehyde, 30 mL of ethanol, RT and 35 W tungsten lamp as light source. [b]Isolated yield. [c]Desired product not obtained. [d]Reaction in dark.

Photocatalytic activity of CdSe/MMT nanocomposite

To optimize reaction conditions, synthesis of 2-phenylbenzothiazole (**3a**) from 2-aminothiophenol and benzaldehyde is chosen as model reaction in ethanol (Table 1). Initially, 5 mg of CdSe NP's is used as photocatalyst that resulted in 48% of **3a** under visible light irradiation within 0.5 h (entry 1). Using nanocomposites (entries 2-4), it is observed that the yield of **3a** has significantly enhanced up to 94% by sequential increase in CdSe loading on MMT with 10% loading (entry 3) found to be adequate with 93% conversion within 0.5 h. Also, 5 mg of catalyst is sufficient to bring about maximum conversion to **3a** (entries 5-7). Moreover, imine intermediate is obtained when reaction is carried out with MMT alone (Supporting information Fig. S4) and further it does not proceed towards formation of **3a**. These results clearly suggested that there exists significant contribution from both homogeneously dispersed CdSe NP's and MMT support that results in efficient conversion through stronger adsorption and photochemical cyclisation in a synergistic manner. Thus, it may be argued that CdSe-MMT composite provides a nano-heterogeneous center for the condensation of aldehyde and amine leading to an imine intermediate that simultaneously undergoes photocyclisation on catalytic surface. After screening different solvents for the photochemical reaction, better yield is obtained with ethanol (Supporting information, Table T1).

With these optimized conditions, we investigated the scope and functional group compatibility of visible-light driven photocatalytic synthesis of 2-substituted benzothiazoles using 2-aminothiophenol (**1)** and aliphatic, aromatic and heterocyclic aldehydes (Table 2). It is noted that formation of benzothiazoles is faster with heterocyclic aldehydes, while larger time is required for aliphatic aldehydes. Such a feature could be ascribed to stronger adsorption tendency of heterocyclic substrates on sites of MMT as compared to aliphatic compounds and consequently this step happens to be crucial towards photocyclization process. These compounds are obtained in good yields (98–83%) within 20 – 55 min. with quantum yields ranging from 32.00–14.55%. Heterocyclic aryl aldehydes possessing either nitrogen or sulfur atom are efficiently converted to the corresponding benzothiazoles (**3j** and **3k**) in excellent yields (Table 2, entry 10 and 11). On the other hand, there seems to be less influence of substituents present on aromatic aldehyde (entries 1-9) where % yield and exposure time is almost similar; however, slight alteration is observed with hydroxyl, methoxy or nitro derivatives (entries 3, 4 & 6). It is reported that during the photochemical synthesis of halo-benzothiazoles, dehalogenation of aldehyde results in the formation of mixtures of the desired product and dehalogenated benzothiazoles.[28] However, CdSe/MMT nanocomposite selectively converts halo-substituted aldehydes to corresponding halo-benzothiazoles (**3g-3i**) without de-halogenation step (entries 7-9). Thus, it may be argued that stronger chemisorption of aldehydes on the catalytic surface induces facile electron transfer thereby promoting radical cyclization of imine intermediate to corresponding cyclic product. Such a tandem process is necessarily occurring because of stronger association of CdSe NP's within MMT matrix that favors photochemical cyclization step in a synergic manner. However, aliphatic aldehyde seems to be less active towards cyclization as this conversion requires almost 60 min (Table 2, entry 12 and 13). Further assessment of photocatalytic activity of CdSe/MMT can be vouched from TON and TOF characteristics which are found to be significantly higher for heterocyclic aldehydes (entry 10 & 11) while lowest values are obtained for aliphatic aldehydes (entry 12 & 13). Within aromatic aldehydes, it is observed that presence of strong adsorbing groups like hydroxyl, methoxy and nitro on clay support favor better conversion with excellent TOF and TON values. Moreover, these values are found to better as compared to dye[27] and CdS[30] catalysed photochemical synthesis of 2-substituted benzothiazoles.

Adopting the same strategy, we have also investigated the potentiality of CdSe/MMT towards photochemical synthesis of 2-substituted benzimidazoles (Table 3) using aliphatic, aromatic and heterocyclic aldehydes with *o*-phenylenediamine. However, this conversion required longer reaction time (1.5 – 3 h) as well as yields are comparatively lower (94–68%) with quantum yields ranging from 8.88 – 4.44%. It is probably due to slower generation of biradical on imine intermediate as a consequence of lesser tendency of amine functionality for radical formation as compared to thiol moiety. As observed earlier, the reactivity of heterocyclic aldehydes is found to be better as compared to aliphatic aldehydes. For example, **2j** and **2k** yielded corresponding benzimidazoles within 1.5 h (entries 3 & 4) while similar time is required for conversion of nitro-aromatic aldeheyde with excellent yield (entry 2). The order of TON and TOF values for different aldehydes used in the synthesis of 2-substituted benzimidazoles is found to heterocyclic > aromatic > aliphatic. We have also explored the photocatalytic efficiency of 10% CdSe/MMT under solar light where the synthesis of benzazoles is carried out under Sunlight (Table 4). The reaction time is found to be comparatively more than visible light with lesser % yields of benzothiazoles (71 – 83) and benzimidazoles (67 – 78). However, these conversions are achieved within shorter

Table 2: Photochemical synthesis of 2-substituted benzothiazoles[a]

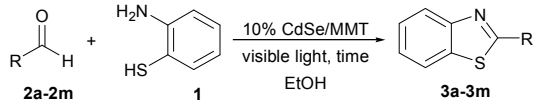

2a-2m 1 3a-3m

Entry	R	Time (min.)	Product	% Yield[b]	TON[c]	TOF (h^{-1})[d]
1	C_6H_5 **2a**	30	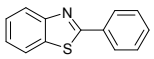 **3a**	93	356	712
2	4-(NMe_2)C_6H_5 **2b**	30	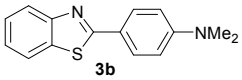 **3b**	95	364	728
3	4-(OH)C_6H_5 **2c**	25	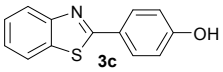 **3c**	94	360	864
4	4-(OMe)C_6H_5 **2d**	25	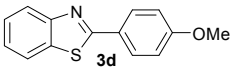 **3d**	95	364	874
5	4-(Me)C_6H_5 **2e**	30	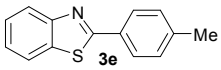 **3e**	93	356	712
6	3-(NO_2)C_6H_5 **2f**	25	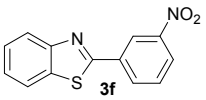 **3f**	96	368	883
7	4-(Cl)C_6H_5 **2g**	30	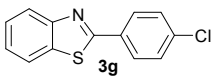 **3g**	92	352	704
8	4-(F)C_6H_5 **2h**	30	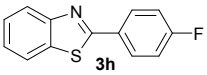 **3h**	91	348	696
9	3-(Br)C_6H_5 **2i**	30	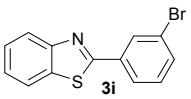 **3i**	90	344	688
10	2-pyridine **2j**	20	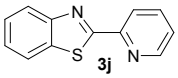 **3j**	98	375	1125
11	2-thiophene **2k**	25	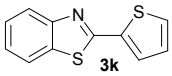 **3k**	96	367	881
12	Me **2l**	40	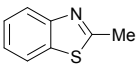 **3l**	87	333	499
13	H **2m**	55	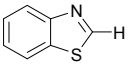 **3m**	83	318	347

[a]Reaction conditions: 10 mmol of 2-aminobenzenethiol, 10 mmol of aldehyde, 5 mg of 10% CdSe/MMT, 30 mL ethanol and RT. [b]Isolated yield. [c]Moles of 2-substituted benzothiazoles formed per mol catalyst. [d]Rate of the formation of 2-substituted benzothiazoles per mol catalyst per unit time.

Table 3: Photochemical synthesis of 2-substituted benzimidazoles[a]

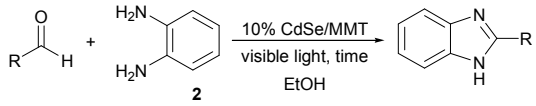

2

Entry	R	Time (h)	Product	% Yield[b]	TON[c]	TOF (h^{-1})[d]
1	C_6H_5 **2a**	2	**4a**	91	348	174
2	3-(NO_2)C_6H_5 **2f**	1.5	**4f**	93	356	257
3	2-pyridine **2j**	1.5	**4j**	94	360	240
4	2-thiophene **2k**	1.5	**4k**	92	352	235
5	Me **2l**	2.5	**4l**	71	272	109
6	H **2m**	3	**4m**	68	318	347

[a]Reaction conditions: 10 mmol of o-phenylenediamine, 10 mmol of aldehyde, 5 mg of 10% CdSe/MMT, 30 mL ethanol and RT. [b]Isolated yield. [c]The moles of 2-substituted benzimidazoles formed per mol catalyst. [d]Rate of the formation of 2-substituted benzimidazoles per mol catalyst per unit time.

Table 4: Solar light driven synthesis of benzazoles[a]

Entry	Aldehyde	Reactant	Time (h)	Product	Isolated Yield (%)
1	2a	1	4	3a	71
2	2f	1	3	3f	78
3	2j	1	2.5	3j	83
4	2a	2	7	4a	67
5	2f	2	6	4f	72
6	2j	2	4	4j	78

[a]Reaction conditions: 10 mmol each of aldehyde and reactant, 5 mg of 10% CdSe/MMT, 50 mL ethanol.

time with less amount of catalyst as compared to those reported in the literature.[28]

Reusability study

The beneficial activity of photocatalyst can be judged from its successive utilization in photochemical reaction; since it is quite likely that catalyst surface undergoes photo-corrosion during continuous exposure to light. This aspect is evaluated for synthesis of 3a and 4a where the catalyst recovered after 1st cycle is used for subsequent four cycles (Fig. 3). It is interesting to note that % yield of these products is not significantly lowered after five cycles. This observation clearly suggests that the catalyst surface remains active even after continuous illumination; although slight lowering in the yield may be due to formation of oxide layer on the surface. Moreover, amount of Cd and Se leached from CdSe/MMT surface after fifth cycle is found to be extremely low (2.6 and 4.7 ppb) implying that our photocatalyst may be used in a continuous process.

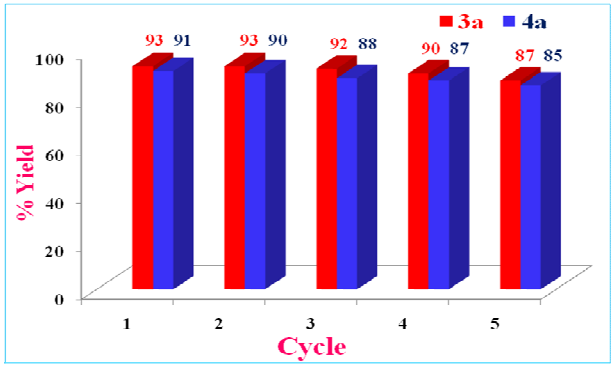

Fig. 3: Reusability studies of 10% CdSe/MMT for synthesis of 2-phenylbenzothiazole (3a) and 2-phenyl benzimidazole (4a)

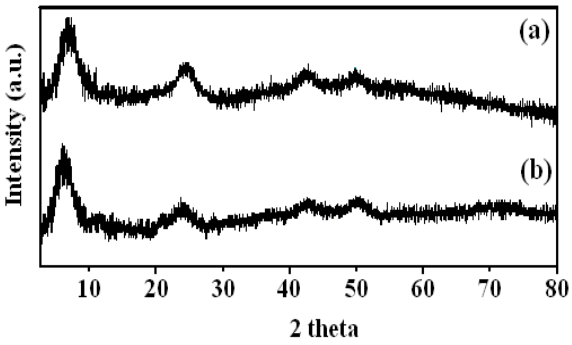

Fig. 4: XRD patterns of 10% CdSe/MMT for (a) fresh (b) after 5 cycles

Evaluation of surface properties

To understand the structural changes that has occurred on the catalyst surface during continuous exposure to visible light, we have carried out post-characterization of recovered

Evaluation of surface properties

photocatalyst after five cycles using XRD, XPS and Raman analysis. It can be seen from XRD pattern of used 10% CdSe/MMT (Fig. 4b) that the peak positions corresponding to Zinc blend structure remains unchanged; although slight broadening is observed for (002) peak probably due to formation of structural defects on the surface induced by absorption of visible light. This feature is further established by XPS analysis, since this technique is useful in identifying (i) elemental composition of the surface (ii) their percentage composition and (iii) exact nature of the respective elements.[33] The deconvoluted Cd features for fresh 10% CdSe/MMT comprises of two main peaks at 405.85 and 412.71 eV due to $3d_{5/2}$ and $3d_{3/2}$ respectively (Fig. 5 a) while the corresponding Se 3d peak is observed at 54.43 eV (Fig. 5 d) which are in concurrent with those reported for bulk CdSe.[34, 35] These characteristics are primarily originating from the presence of different chemical species of Cd and Se on the nanocomposite surface. For example, the nature Cd present on the surface of the catalyst can be of two types: (i) Cd bound to Se (Cd_a) and (ii) Cd bound to other elements (Cd_b).[36] With this assumption, we have estimated the Cd_b/Cd_a ratio from the integrated Cd 3d signal intensities for fresh and reused 10% CdSe/MMT composite (Supporting information Table T2). For fresh catalyst, this ratio is found to be 0.49 that drastically changed to 2.2 for used catalyst which indicates that the surface of reused nanocomposite is approximately four times richer with Cd ions bound to other atoms. Moreover, the oxygen content of used catalyst ($CdSe_{0.31}O_{0.69}$) is almost doubled as compared to fresh catalyst ($CdSe_{0.67}O_{0.33}$) implying the formation of thin layer of CdO due to light induced surface oxidation of the catalyst.[37] This phenomenon is further substantiated by analyzing oxygen region. The oxygen content mainly arises from (i) adsorbed water, (ii) surface hydroxyl groups on MMT and (iii) oxide which are observed at 531.6, 533.4 and 532.6 eV respectively. Out of these, third peak is ascribed to formation of CdO layer whose intensity (Supporting information Figure S5) is increased by almost two times for used catalyst at the

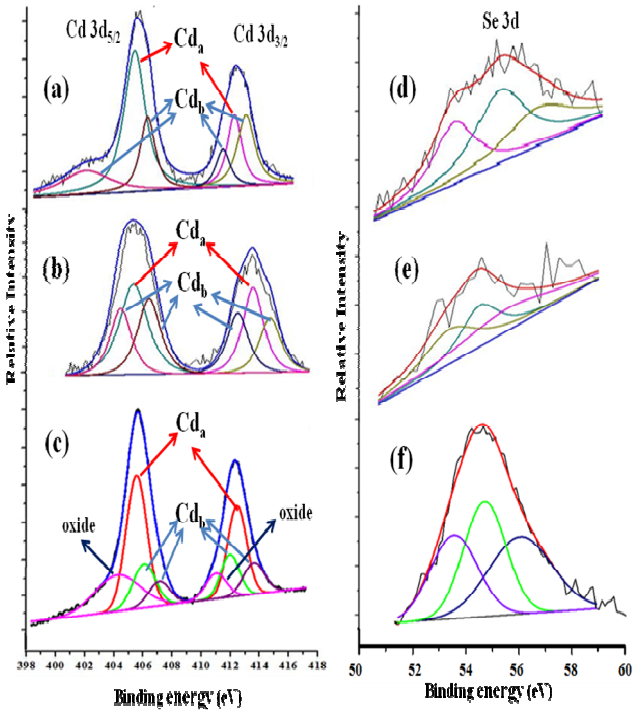

Fig. 5: XPS spectra of Cd and Se regions (a, d) before and (b, e) after 5 cycles as well as calcined CdSe/MMT (c, f). Cd peaks are characterized as Cd bound to Se (Cd_a) and Cd bound to oxygen (Cd_b).

expense of decrease in the intensity for peak corresponding to absorbed water. Thus, it may be argued that during photochemical process, CdSe surface is continuously oxidized during successive cycles that result in development of mixed phase on the catalyst surface that comprises of n-type CdSe and p-type CdO species. This leads to generation of p-n type of hetero-junction on the catalyst surface where continuous flow of electrons from CdSe core to this junction results in retaining the photocatalytic activity even after five successive cycles. To further address this aspect, we have calcined fresh 10% CdSe/MMT at 100°C for 3 h and the residue thus obtained is evaluated for its photocatalytic activity towards the synthesis of **3a**. It is observed that its yield is decreased by 20% implying that oxide layer indeed influence the photocatalytic activity of CdSe/MMT nanocomposites. Moreover, XPS analysis of the calcined photocatalyst revealed the presence of additional peak (Fig. 5 c) corresponding to Cd bound to oxygen as well as the oxygen content is found to be almost same (Supporting information Fig. S5 c) as that used catalyst. It implies that the presence of thin layer of CdO on CdSe also passivates the surface defects as well as immobilizes these charge carriers within CdSe core[38, 39] that accounts for better photostability and excellent photocatalytic efficiency of CdSe/MMT nanocomposite.

CdSe nanoparticles exhibit two characteristic Raman peaks corresponding to longitudinal-optical mode and 2LO photon scattering at 208 and 431 cm^{-1} respectively.[40] Upon nanocomposite formation with MMT, the former peak remains unaltered while the later peak is shifted to lower energy side

Table 4: Phototcatalytic efficiency of different heterogeneous photocatalyst towards synthesis of imidazoles, thiazoles and oxazoles

Catalyst	Product	Amt. (mg)	Source	Time (h)	% yield	Ref.
mpg-C_3N_4	oxazole	50	λ > 420 nm	5	70 – 90[a]	29
	imidazole			4 – 5.5	97 – 99[b]	
	thiazole			4 – 5.5	91 – 97[c]	
Ag- and Pt-doped TiO_2	imidazole	25	Solar Light	4	86 – 98[d]	31
Pt-doped TiO_2	imidazole	80	λ > 300 nm	4 - 24	82 – 99[e]	32
CdS Nanosphere	thiazole	5	Xenon Lamp 300 W; λ > 420 nm	0.3 – 1.5	60 – 98[d]	30
10% CdSe/MMT	Thiazole	5	Tungsten Lamp	0.3 – 0.9	83 – 98[d]	Present work
	imidazole		35 W; λ > 420 nm	1.5 - 3	68 – 94[d]	

[a]By GC analysis with 24 – 75% selectivity. [b]By GC analysis with 91 – 98% selectivity. [c] By GC analysis with 92 - 97% selectivity. [d]Isolated yields. [e]GC yield.

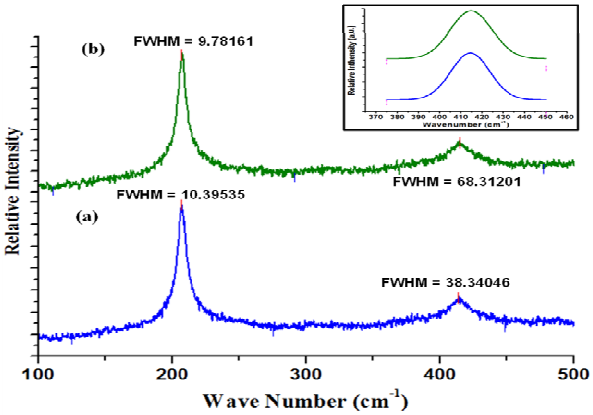

Fig. 6: Raman spectra of (a) fresh and (b) reused 10% CdSe/MMT. Inset: expanded view of peak at 413 cm^{-1}.

(413 cm^{-1}) with broadened nature due to relaxation of momentum conservation as a consequence of homogeneous dispersion of CdSe NP's within MMT matrix (Fig. 6 a). Although the position of both these bands for reused catalyst does not undergo any significant change, peak broadening is observed with 2LO photon peak (Fig. 6 b). This change is evaluated from FWHM of fresh (Fig. 6 a) and recycled photocatalyst (Fig. 6 b) wherein it is observed that there exists significant enhancement for FWHM (by 30 cm^{-1}) with 2LO photon peak. Such a feature can be ascribed to passivation of the photocatalyst surface due to formation of Raman inactive thin layer of CdO on CdSe core. It implies that longitudinal oscillations on the catalyst surface are responsible for negative photon dispersion that ultimately retains the photocatalytic activity even after continuous exposure to light.[41] Thus, it may be argued that modification of CdSe/MMT catalyst after continuous exposure to light results in the formation of robust p-n junction through passivation of surface structural defects. These features account for better photostability and excellent photocatalytic efficiency of CdSe/MMT nanocomposites afforded by synergism in CdSe and MMT structures.

To highlight our work, we have compared the photocatalytic activity of different heterogeneous photocatalysts that are explored for the synthesis of benzimidazoles and benzothiazoles under visible light (Table 4). Inspection of this table reveals that these conversions are achieved at reasonably higher irradiation time either with high power or solar light and high catalyst loading[29-32] while 10% CdSe/MMT exhibit excellent photocatalytic activity with good yields in less time. The isolated yields are reported for Ag and Pt-doped TiO_2 where reaction time and catalyst loading is significantly higher as compared to our photocatalyst.[31] Although, appropriate comparison can made with unsupported CdS nanosphere,[30] synthesis of only benzothiazoles is reported with 5 mg of catalyst and high wattage Xenon lamp. It implies that 10% CdSe/MMT photocatalyst exhibit excellent photocatalytic properties due to; (a) stronger light absorption capability of CdSe sites that are uniformly dispersed in MMT structure (b) Lewis acidity of MMT is beneficial for better adsorption of reactants and (c) synergistic association of CdSe and MMT leads to formation of bifunctional nature of photocatalyst. These features are further corroborated with formation of photoresponsive p-n junction that accounts for recycling capability of this nanocomposite.

The plausible mechanism of visible light induced synthesis of imidazoles and thiazoles is outlined in Scheme 1. This process consists of three steps: (i) formation of imine intermediate (ii) radical generation and subsequent cyclization and (iii) aerobic oxidation of cyclized intermediate. Since first step normally requires an acidic condition, it is observed that acidic sites present on MMT are beneficial for imine (I) formation through adsorptive association of amine and aldehyde on catalyst surface. Visible light induced generation of radicals is known to be critical and rate determining step that affects overall conversion to desired product. In our case, formation of

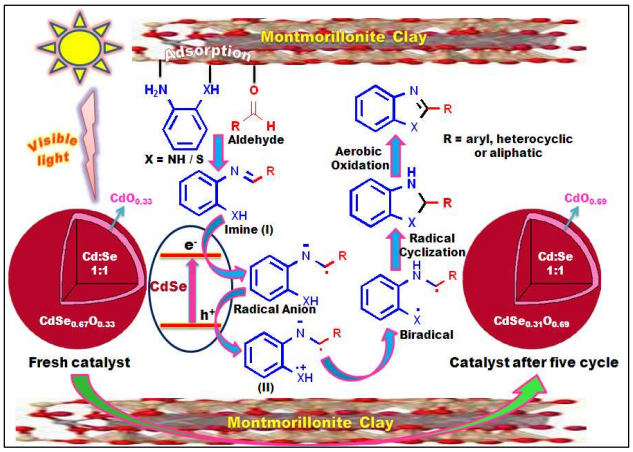

Scheme 1: A plausible mechanism for photocatalytic synthesis of 2-substituted benzothiazoles and benzimidazoles.

radicals seems to be easier due to presence of n-type CdSe sites where electron transfer from CdSe to adsorbed imine intermediate is supposed to be faster. Moreover, the stabilization of radical (II) is essential as it accounts for better yield in lesser time. Although generation of radical on imine functionality seems to occur in almost identical manner for both imidazoles and thiazoles, creation of radical on thiol and amine centers is the key factor towards formation of their respective products. Since generation of radical and its stabilization is easier with sulphur center, the formation of benzothiazoles is achieved in lesser time with good yields. Also, radical cation (II) generation on sulphur and subsequent absorption of liberated electrons by positively charged holes (h^+) contributes for improved rate of photochemical reaction. On the other hand, formation of biradical on benzimidazole intermediate seems to be less favored and time dependent, longer reaction times are required for the photochemical synthesis of benzimidazoles. Thus, it may be argued that formation of biradicals on imine intermediates is more pronounced for thiol as compared to amine which is driven by electron donor n-type CdSe sites present on photocatalytic surface. Finally, the aerobic oxidation is essential for the formation of heterocyclic compound as we could not obtain desired product under oxygen free (inert) condition; rather imine intermediate is obtained (Supporting information Fig. S6). This observation has also reported for the synthesis of benzothiazoles.[28b]

Conclusions

In summary, we have developed a simple, facile and environmental benign methodology for the synthesis of 2-substituted benzimidazoles and benzothiazoles under visible light using nano-engineered CdSe/MMT as a photocatalyst. The versatility of these nanocomposites can be ascertained by radical cyclization of imine intermediates formed with aliphatic, aromatic and heterocyclic aldehydes at faster rates through efficient absorption of visible light. This behavior is reflected in its repetitive usage where the catalytic activity is marginally reduced during five successive cycles even after prolonged exposure to light. It is established that photocorrosion is inhibited due to generation of thin layer of CdO on the catalyst surface where structural defects of zinc blend structure of CdSe is passivated *via* formation of p-n heterojunction on catalyst surface. These features are manifested due to synergistic interaction between CdSe sites and MMT support within nanocomposite structure. Thus, the present work clearly demonstrates that photochemical process for synthesis of biologically active scaffolds can be achieved by the principles of green chemistry by employing renewable resources like visible light, air, and an environmentally benign solvent in a highly atom-economical and energy-efficient manner.

Acknowledgements

Authors are thankful to Principal, Abasaheb Garware College, for providing infrastructure, support and constant encouragement. We sincerely thank Dr. K. R. Patil and Dr. S. P. Gokhale, NCL, Pune for providing XPS and Raman spectra. We are pleased to acknowledge Dr. Brijesh Kadu and Mr. Alok Jakhade for processing and constructive suggestions of XPS spectra as well as Mr. Dattatraya S. Shinde for providing NMR spectra. ARW is thankful to CSIR, New Delhi for providing SPM fellowship. Authors are thankful to DST-FIST for providing infrastructural grant through FIST program.

References

1 (a) C. K. Prier, D. A. Rankic and D. W. C. MacMillan, *Chem. Rev.,* 2013, **113**, 5322–5363; (b) N. Hoffmann, *Chem. Rev.,* 2008, **108**, 1052; (c) M. Fagnoni, D. Dondi, D. Ravelli and A Albini, *Chem. Rev*., 2007, **107**, 2725–2756.
2 X.Lang, X. Chen and J. Zhao, *Chem. Soc. Rev.*, 2014, **43**, 473-486.
3 (a) D. Ravelli, D. Dondi, M. Fagnoni and A. Albini, *Chem. Soc. Rev.***,** 2009, **38**, 1999-2011; (b) T. P. Yoon, *ACS Catal.*, 2013, ***3***, 895–902.
4 (a) S. Dong, J. Feng, M. Fan, Y. Pi, L. Hu, X. Han, M. Liu, J. Sun and J. Sun , *RSC Adv.,* 2015, **5**, 14610-14630. (b) K. Kabra, R. Chaudhary and R. L. Sawhney, *Ind. Eng. Chem. Res.*, 2004, **43,** 7683–7696; (c) M. R. Hoffmann, S. T. Martin, W. Choi and D. W. Bahnemann, *Chem. Rev.,* 1995, **95**, 69; (d) J. Song, Z. Luo, D. K. Britt, H. Furukawa, O. M. Yaghi, K. I. Hardcastle and C. L. Hill, *J. Am. Chem. Soc.*, 2011, **133**, 16839-16846.
5 (a) T. Hisatomi, J. Kubota and K. Domen, *Chem. Soc. Rev.,* 2014, **43**, 7520-7535; (b) M. G. Walter, E. L. Warren, J. R. McKone, S. W. Boettcher, Q. Mi, E. A. Santori and N. S. Lewis, *Chem. Rev.*, 2010, **110,** 6446–6473; (c) F. Song, Y. Ding, B. Ma, C. Wang, Q. Wang, X. Du, S. Fua and J. Song, *Energy Environ. Sci*., 2013, **6**, 1170–1184.
6 Y. Ma, X. Wang, Y. Jia, X. Chen, H. Han and C. Li, *Chem. Rev.*, 2014, **114**, 9987–10043.
7 (a) J. Wu, Z. Lan, J. Lin, M. Huang, Y. Huang, L. Fan, and G. Luo, *Chem. Rev.*, 2015, **115**, 2136–2173; (b) Q. Zhang, E. Uchaker, S. L. Candelaria and G. Cao, *Chem. Soc. Rev.*, 2013, **42**, 3127-3171.
8 S. Tang, K. Liu, C. Liu and A. Lei, *Chem. Soc. Rev.***,** 2015, **44,** 1070-1082.

9 (a) C. S. Yeung and V. M. Dong, *Chem. Rev.*, 2011, **111**, 1215–1292; (b) C. Liu, H. Zhang, W. Shi and A. Lei, *Chem. Rev.,* 2011, **111**, 1780–1824; (c) M. Fagnoni, D. Dondi, D. Ravelli and A. Albini, *Chem. Rev.,* 2007, **107**, 2725–2756.
10 (a) E. N. Gulakova, D. V. Berdnikova, T. M. Aliyeu, Y. V. Fedorov, I. A. Godovikov and O. A. Fedorova, *J. Org. Chem.*, 2014, **79**, 5533–5537; (b) F. Su, S. C. Mathew, L. Möhlmann, M. Antonietti, X. Wang and S. Blechert, *Angew. Chem., Int. Ed.,* 2011, **50**, 657–660; (c) J. H. Park, K. C. Ko, E. Kim, N. Park, J. H. Ko, D. H. Ryu, T. K. Ahn, J. Y. Lee and S. U. Son, *Org. Lett.,* 2012, **14**, 5502–5505; (d) A. J. Musacchio, L. Q. Nguyen, G. H. Beard and R. R. Knowles, *J. Am. Chem. Soc.*, 2014, **136**, 12217–12220.
11 (a) V. P. Srivastava, A. K. Yadav and L. D. S. Yadav, *Synlett,* 2013, **24**, 465–470. (b) A. K. Yadav and L. D. S. Yadav, *Org. Biomol. Chem.,* 2015, **13**, 2606-2611.
12 (a) B. Chen, J. R. G. Evans, H. C. Greenwell, P. Boulet, P. V. Coveney, A. A. Bowden and A. Whiting, *Chem. Soc. Rev.*, 2008, **37**, 568-594; (b) J. Zhu, M. Chen, Q. He, L. Shao, S. Wei and Z. Guo, *RSC Adv.,* 2013, **3**, 22790-22824; (c) F. de Clippel, M. Dusselier, S. V. de Vyver, L. Peng, P. A. Jacobs and B. F. Sels, *Green Chem.*, 2013, **15**, 1398-1430.
13 M. Kotkata, A. Masoud, M. Mohamed and E. Mahmoud, *Phys. E,* 2009, **41**, 640–645.
14 (a) H. Koyuncu, *Appl. Clay Sci.,* 2008, **38**, 279–287; (b) Z. Qian, G. Hu, S. Zhang and M. Yang, *Phys. B,* 2008, **403**, 3231–3238; (c) B. Hu and H. Luo, *Appl. Surf. Sci.,* 2010, **257**, 769–775.
15 (a) D. Kumar, M. R. Jacob, M. B. Reynolds and S. M. Kerwin, *Bioorg. Med. Chem.*, 2002, **10**, 3997−4004; (b) W. A. Denny, G. W. Rewcastle and B. C. Bauley, *J. Med. Chem.*, 1990, **33**, 814−819.
16 T. T. Güngör, A. Fouquet, J. M. Eulon, D. Provost, M. Cazes and A. Cloarec, *J. Med. Chem.,* 1992, **35**, 4455−4463.
17 (a) A. R. Porcari, R. V. Devivar, L. S. Kucera, J. C. Drach and L. B. Townsend, *J. Med. Chem.,* 1998, **41**, 1252−1262; (b) T. Roth, M. L. Morningstar, P. L. Boyer, S. H. Hughes, R. W. Buckheitjr and C. J. Michejda, *J. Med. Chem.,* 1997, **40**, 4199−4207.
18 E. Seyhan, N. Sultan, A. Nilgun and N. Noyanalpan, *Arzneim.-Forsch.,* 1997, **47**, 410−412.
19 N. Azizi, A. K. Amiri, R. Baghi, M. Bolourtchian and M. H. Hashemi, *Monatsh. Chem.*, 2009, **140**, 1471-1473.
20 J. R. Mali, D. V. Jawale, B. S. Londhe and R. A. Mane, *Green Chem. Lett. Rev.,* 2010, **3**, 209−212.
21 G. F. Chen, H. M. Jia, L. Y. Zhang, B. H. Chen and J. T. Li, *Ultrason. Sonochem.*, 2013, **20**, 627-792.
22 R. R. Nagawade and D. B. Shinde, *Russ. J. Org. Chem.,* 2006, **42**, 453−454.
23 (a) H. Jin, X. Xu, J. Gao, J. Zhong and Y. Wang, *Adv. Synth. Catal.,* 2010, **352**, 347−350; (b) M. A. Chari, D. Shobha and T. Sasaki, *Tet. Lett.,* 2011, **52**, 5575−5580.
24 E. Verner, B. A. Katz, J. R. Spencer, D. Allen, J. Hataye, W. Hruzewicz, H. C. Hui, A. Kolesnikov, Y. Li, C. Luong, A. Martelli, K. Radika, R. Rai, M. She, W. Shrader, Sprengeler, P. A.; S. Trapp, J. Wang, W. B. Young and R. L. Mackman, *J. Med. Chem.,* 2001, **44**, 2753−2771.
25 R. Ruiz, A. Corma, M. J. Sabater, *Tetrahedron*, 2010, **66**, 730−735.
26 M. Jafarpour, A. Rezaeifard, M. Ghahramaninezhad and T. Tabibi, N*ew J. Chem.,* 2013, **37**, 2087-2095.
27 S. Samanta, S. Das and P. Biswas, *J. Org. Chem.*, 2013, **78**, 11184−11193.
28 (a) Y. Cheng, J. Yang, Y. Qu, and P. Li, *Org. Lett.,* 2012, **14**, 98-101; (b) L. Wang, Z.G. Ma, Z.J. Wei, Q.Y. Meng, D.T. Yang, S.F. Du, Z.F. Chen, L.Z. Wu and Q. Liu, *Green Chem.*, 2014, **16**, 3752-3757.
29 F. Su, S. C. Mathew, L. Mohlmann, M. Antonietti, X. Wang and S. Blechert, *Angew. Chem. Int. Ed.,* 2011, **50,** 657–660.
30 S. Das, S. Samanta, S. K. Maji, P. K. Samanta, A. K. Dutta, D. N. Srivastava, B. Adhikary and P. Biswas, *Tet. Lett.,* **54**, 2013, 1090–1096.
31 K. Selvam, B. Krishnakumar, R. Velmurugan, M. Swaminathan, *Catal. Commun.,* 2009, **11**, 280–284.
32 Y. Shiraishi, Y. Sugano, S. Tanaka and T. Hirai, *Angew. Chem. Int. Ed.*, 2010, **49**, 1656 –1660.
33 C. D. Wagner, W. M. Riggs, L. E. Davis, J. F. Moulder and G. E. Muilenberg, *Handbook of X-ray Photoelectron Spectroscopy;* Physical Electronics Division, Perkin-Elmer: Eden Prairie, MN; 1979.
34 C. J. Vesely and D. W. Langer, *Phys. Rev.*, 1971, **B4**, 451–462.
35 J. E. B. Katari, V. L. Colvin, A. P. Alivisatos, *J. Phys. Chem.*, 1994, **98**, 4109−4117.
36 K. B. Subila, G. K. Kumar, S. M. Shivaprasad and K. G. Thomas, *J. Phys. Chem. Lett.,* 2013, **4,** 2774−2779.
37 Y. Park, M. J. Felipe and R. C. Advincula, *ACS Appl. Mater. Interfaces,* 2011, **3**, 4363–4369.
38 B. O. Dabbousi, J. Rodriguez-Viejo, F. V. Mikulec, J. R. Heine, H. Mattoussi, R. Ober, K. F. Jensen and M. G. Bawendi, *J. Phys. Chem. B*, 1997, **101**, 9463−9475.
39 X. Peng, M. C. Schlamp, A. V. Kadavanich and A. P. Alivisatos, *J. Am. Chem. Soc.,* 1997, **119**, 7019−7029.
40 F. Widulle, S. Kramp, N. Pyka, A. Gobel, T. Ruf, A. Debernardi, R. Lauck and M. Cardona, *Phys. B,* 1999, **263,** 448–451.
41 R. C. Chikate, B. S. Kadu and M. A. Damle, *RSC Adv.,* 2014, **4**, 35997–36005.

Graphical Abstract:

Synergism in CdSe/MMT photocatalyst induces efficient synthesis of 2-substituted benzazoles under visible light with excellent yields and recycling capability.